Nousiainen, Kari; Intosalmi, Jukka; Lähdesmäki, Harri

A Mathematical Model for Enhancer Activation Kinetics During Cell Differentiation

Published in:
Algorithms for Computational Biology - 6th International Conference, AlCoB 2019, Proceedings

DOI:
10.1007/978-3-030-18174-1_14

Published: 01/01/2019

Document Version
Publisher's PDF, also known as Version of record

A Mathematical Model for Enhancer Activation Kinetics During Cell Differentiation

Kari Nousiainen[1][0000−0001−5484−7934], Jukka Intosalmi[1][0000−0002−5262−1701], and Harri Lähdesmäki[1]

Department of Computer Science, Aalto University School of Science, FI-00076 Aalto, Finland
kjnousia@gmail.com

Abstract. Cell differentiation and development are for a great part steered by cell type specific enhancers. Transcription factor (TF) binding to an enhancer together with DNA looping result in transcription initiation. In addition to binding motifs for TFs, enhancer regions typically contain specific histone modifications. This information has been used to detect enhancer regions and classify them into different subgroups. However, it is poorly understood how TF binding and histone modifications are causally connected and what kind of molecular dynamics steer the activation process.
Contrary to previous studies, we do not treat the activation events as static epigenetic marks but consider the enhancer activation as a dynamic process. We develop a mathematical model to describe the dynamic mechanisms between TF binding and histone modifications known to characterize an active enhancer. We estimate model parameters from time-course data and infer the causal relationships between TF binding and different histone modifications. We benchmark the performance of this framework using simulated data and survey the ability of our method to identify the correct causal mechanisms for a variety of system dynamics, noise levels and the number of measurement time points.

Keywords: dynamic modeling · enhancer activation · cell differentiation

1 Introduction

Cell differentiation is steered by highly complex molecular machinery which controls the execution of cell type specific transcriptional programs. Transcriptional programs are typically initiated by external signaling molecules which bind receptors on the cell surface and activate downstream signaling pathways. Signaling cascades in turn activate lineage determining transcription factors that bind selected regions in the genome and control the regulatory functions of these regions, for instance, by modifying the structure of chromatin. An important class of genomic regions bound by lineage specifying transcriptions factors are so-called enhancer regions which facilitate DNA looping, and as a consequence, enable interaction between enhancer and promoter sequences leading to the initiation of

transcription [24, 7]. Systematic activation of these selected regulatory regions is an important part of lineage determine supervision, but the detailed molecular kinetics behind these epigenetic mechanisms are poorly understood [16]. Modern high-throughput measurement techniques, such as chromatin immunoprecipitation sequencing, provide practical means to observe the epigenetic states in different cell types. Such methods have vigorously been used to determine global chromatin markings across different cell types. Further, new insights on the molecular mechanisms can be gained by analyzing these data using computational approaches.

Computational methods that have been used to study epigenetic mechanisms include, for instance, Bayesian networks, sparse partial correlation networks and maximum entropy framework [13, 12, 18, 26]. Yu et al. [25] have also combined gene expression data analysis with histone modification networks and theoretical investigations of histone modification networks have also been proposed in [9]. Even though these existing approaches provide invaluable information about the structure of epigenetic signaling networks, the approaches are limited in the sense that they provide only a static view on the network structure and do not account for dynamic causative relationships between epigenetic modifications. In other words, these approaches provide information about statistical dependencies between measured quantities but are incapable of capturing mechanistic features of the underlying system. Dynamic view on epigenetic signaling is especially important when considering cell differentiation processes which depend on enhancer activity.

During cell differentiation processes, the state of an enhancer typically changes transiently from an inactive state to an active state. The activation process is steered by enzymatic signals (readers and writers of histone modifications) accompanied with appropriate transcription factor activities [2]. Consequently, in order to learn dynamic behavior leading to active enhancer state, it is necessary to quantify the dynamic and causative relationships between the key components of this complex molecular system.

In this study, we take the first steps towards mechanistic analysis of epigenetic signaling events that lead to the enhancer activation. We construct a mechanistic ordinary differential equation model to describe central histone modification and transcription factor dynamics leading to active enhancer state and apply this model to study enhancer activation during human T helper 2 (Th2) cell differentiation. Our model is designed to capture the dynamics of histone H3 lysine 4 monomethylation (H3K4me1), histone H3 lysine 27 acetylation (H3K27ac), and an activating TF. Highly enriched levels of histone modifications H3K4me1 [10] and H3K27ac [3] are known to characterize the active enhancer state in Th2 cells and for example STAT6 is a central transcription factor driving the differentiation into Th2 lineage [17]. To carry out the analysis in a data driven manner, we embed the causal model into a statistical framework which makes it possible to infer the model structure as well as parameters from experimental data. Our result show that experimental data from as few as five time point is sufficient to distinguish cascade of enhancer activation events.

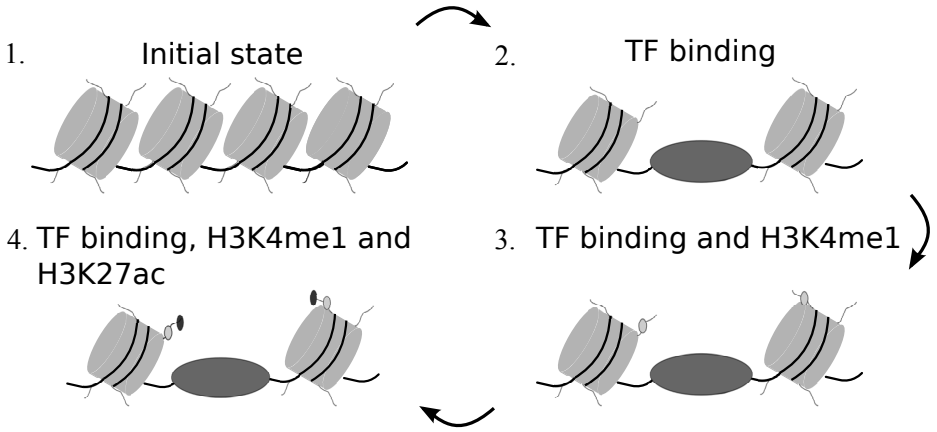

Fig. 1. A possible pathway model of chromatin changes during enhancer activation that are reflected by the abundance data.

2 Methods

2.1 Mathematical Model

The STAT family of transcription factors plays a crucial role in the enhancer activation as well as in the differentiation of Th cells in general [23]. TF is one of the transcritption factors that initiate and steer the differentiation process towards Th2 lineage [14]. One such scenario leading to enhancer activation is illustrated in Figure 1. Initially, there are no TFs bound to the enhancer site and the enhancer associated histone modifications are absent (Figure 1, initial state 1). As the first step, enhancer activation is initiated by TF that binds the enhancer (Figure 1, state 2) and, in the considered scenario, TF binding is first followed by H3K4me1 (Figure 1, state 3) and then finally by the third activation event H3K27ac (Figure 1, state 4). This chain of three causative activation steps leads to active enhancer state and if the underlying assumptions of the causal relationships between the key components are correct, we can build a dynamic model for the activation process by using ODEs that describe the key components.

Because TF activation is driven by T cell activation as well as inducing cytokine signals, we can simply assume that there is a persistent input signal affecting TF. Thus, TF dynamics can be described by the ordinary differential equation

$$\frac{d\,[\mathrm{TF}]}{dt} = \alpha_{\mathrm{TF}} - \delta_{\mathrm{TF}}[\mathrm{TF}], \tag{1}$$

where α_{TF} and δ_{TF} are unknown association and dissociation rate constants of TF and [TF] represent the TF abundance at the enhancer site. Further, if we assume that enzymatic signals that cause the methylation of the histone tail H3K4me1 result from TF binding, we can model H3K4me1 enrichment at the

enhancer cite by means of the equation

$$\frac{d[\text{H3K4me1}]}{dt} = \alpha_{\text{me}}[\text{TF}] - \delta_{\text{me}}[\text{H3K4me1}], \tag{2}$$

where α_{me} and δ_{me} are unknown methylation and demethylation rate constants and [H3K4me1] represent the H3K4me1 abundance at the enhancer site. Similarly, if H3K27ac is driven by H3K4me1 driven enzymatic signals, its enrichment [H3K27ac] at the site can be modeled using the differential equation

$$\frac{d[\text{H3K27ac}]}{dt} = \alpha_{\text{ac}}[\text{H4K3me1}] - \delta_{\text{ac}}[\text{H3K27ac}], \tag{3}$$

where α_{ac} and δ_{ac} are unknown acetylation and deacetylation rate constants. If the causative relationships between the key component TF, H3K4me1, and H3K27ac are correct, the resulting ODE system can be used to approximate the complex molecular kinetics consisting, for example, of TF binding events, enzymatic signals, methylation, acetylation etc.

The approximative model that we derive above indicates that the TF signal drives H3K4me1 which, in turn, drives H3K27ac. In other words, we have a cascade of causative events leading to the active enhancer state and this can be denoted by writing

$$\text{TF binding} \rightarrow \text{H3K4me1} \rightarrow \text{H3K27ac}.$$

However, because the detailed kinetics remain unknown, we cannot be sure if the causative relationships are correct. In other words, the true order of the activation events in the cascade can be, for instance,

$$\text{H3K4me1} \rightarrow \text{TF binding} \rightarrow \text{H3K27ac}.$$

Additionally, some of the activating events can also be synergistic in nature. For example, TF binding and H3K4me1 can drive H3K27ac in a manner which is either additive or multiplicative. These synergistic models can be defined formally using the following equations

$$\frac{d[\text{H3K27ac}]}{dt} = \alpha_{\text{ac1}}[\text{TF}] + \alpha_{\text{ac2}}[\text{H3K4me1}] - \delta_{\text{ac}}[\text{H3K27ac}], \tag{4}$$

and

$$\frac{d[\text{H3K27ac}]}{dt} = \alpha_{\text{ac}}[\text{TF}][\text{H3K4me1}] - \delta_{\text{ac}}[\text{H3K27ac}]. \tag{5}$$

All different scenarios that can be derived by altering the order or the type of the activation steps can be modeled using the rate equations given in Equations 1-5. Altogether there are 13 effectively different alternative models (see Table 1.). Importantly, all these alternative scenarios result in different dynamics of the model output. Further, the dynamics of the model output can be directly linked to observed time-course data and, by means of quantitative statistical methods, it is possible to infer the most likely causative relationships between the key components leading to enhancer activation.

Table 1. A $\perp\!\!\!\perp$B denotes that events A and B are independent; A $\rightarrow$ B denotes that A regulates B; (A $\vee$ B) denotes A or B; (A $\wedge$ B) denotes A and B.

index	type of interaction	order of events
0	independent	H3K4me1 $\perp\!\!\!\perp$H3K27ac $\perp\!\!\!\perp$TF binding
1	cascade	H3K27ac $\rightarrow$ H3K4me1 $\rightarrow$ TF binding
2	cascade	H3K27ac $\rightarrow$ TF binding $\rightarrow$ H3K4me1
3	cascade	H3K4me1 $\rightarrow$ H3K27ac $\rightarrow$ TF binding
4	cascade	H3K4me1 $\rightarrow$ TF binding $\rightarrow$ H3K27ac
5	cascade	TF binding $\rightarrow$ H3K27ac $\rightarrow$ H3K4me1
6	cascade	TF binding $\rightarrow$ H3K4me1 $\rightarrow$ H3K27ac
7	multiplicative synergy	(H3K4me1 $\wedge$ H3K27ac) $\rightarrow$ TF binding
8	multiplicative synergy	(H3K4me1 $\wedge$ TF binding) $\rightarrow$ H3K27ac
9	multiplicative synergy	(H3K27ac $\wedge$ TF binding) $\rightarrow$ H3K4me1
10	additive	(H3K4me1 $\vee$ H3K27ac) $\rightarrow$ TF binding
11	additive	(H3K4me1 $\vee$ TF binding) $\rightarrow$ H3K27ac
12	additive	(H3K27ac $\vee$ TF binding) $\rightarrow$ H3K4me1

2.2 Statistical Framework

We combine the dynamic ODE models with time-course data by means of statistical modeling. More specifically, we set up a statistical framework for the ODE models by using Bayesian methodology as outlined in [8] and carry out posterior inference for the parameters and for the most likely causative relationships between the key components steering enhancer activation [6] (alternative models are listed in Table 1). In the following, we describe the details of our statistical framework.

Let us denote the output of the model M_k by $\boldsymbol{\phi}_{M_k}(\boldsymbol{\theta}_k, t) \in \mathbb{R}^N$ where N is the number of components in the model, $\boldsymbol{\theta}_k$ is the vector of parameters of the model and t is the time point. Further, θ_{kl} is the l'th element of $\boldsymbol{\theta_k}$. Also, let $\mathcal{D} = (y_{11}, \ldots, y_{NT})$ be the experimental data which consists of measurements y_{ij} of the components $i = 1, \ldots, N$ at the time points $t = 1, \ldots, T$. Accordingly, $\phi_{ik}(\boldsymbol{\theta_k}, t_j)$ is the is i'th element at j'th time point of the model output. By assuming normal errors, we define likelihood as

$$p(\mathcal{D} \mid M_k, \boldsymbol{\theta}_k) = \prod_{i=1}^{N} \prod_{j=1}^{T} \mathcal{N}(y_{ij} \mid \phi_{ik}(\boldsymbol{\theta_k}, t_j), \sigma_k^2)$$

where $\mathcal{N}$ is the normal probability density function with mean $\phi_{ik}(\boldsymbol{\theta_k}, t_j)$ and variance σ_k^2. Posterior distribution of the model M_k is

$$p(M_k \mid \mathcal{D}) \propto p(\mathcal{D} \mid M_k)\pi(M_k)$$

or

$$\log(p(M_k \mid \mathcal{D})) = \log(p(\mathcal{D} \mid M_k)) + \log(\pi(M_k)) + C$$

where $\pi(M_k)$ is the prior distribution for the model M_k and C is constant. The marginal likelihoods

$$p(\mathcal{D} \mid M_k) = \int p(\mathcal{D} \mid M_k, \boldsymbol{\theta}_k)\pi(\boldsymbol{\theta}_k \mid M_k)d\boldsymbol{\theta_k}$$

is used to compare models with respect to each other. It can be approximated in many ways [4]. In this study, we apply Laplace approximations (as described e.g. [1]). Assuming uniform prior distribution for the models, i.e. prior probabilities $\pi(M_k)$ are equal, for all $k = 0, \ldots, 12$, we obtain Bayesian information criterion [21] defined by

$$BIC = \log(p(D \mid \hat{\theta}_k, M_k)) - \frac{1}{2}k_0 \log(n),$$

where $p(D \mid \hat{\theta}_k, M_k)$ is the maximum likelihood for model M_k, k_0 is the number of parameters and n is the number of observations.

2.3 Computational Implementation

In this work, we applied tools and methods reported being successful in dynamical modeling in systems biology. The ODE models and the model selection were implemented in Matlab (The MathWorks Inc., Natick, MA, USA) by using PESTO toolbox [22] for parameter optimization and AMICI toolbox [5] for solving the ODE systems numerically. Maximum likelihood estimates for parameters were obtained by employing the sensitivity equations in combination with a multi-start strategy based on latin hypercube sampling as suggested in [19, 20]. We optimized the parameters by maximizing the log-likelihood function from 100 starting points with interior-point algorithm in Matlab's fmincon function.

3 Results

3.1 Evaluation of Model Identifiability and Discrimination

In practice, time-course measurements for histone modifications and TF binding can be carried out only at a few time points. Being aware of the limited size of real data sets, we use a small number of time-points also in our experiments with simulated data. In these experiments, we consider three different scenarios for measurements time-point selection, in the first one the samples are collected at three time points (0, 4 and 72 hours), in the second one the samples are collected at four time points (0, 4, 8, and 72 hours), and in the third samples are collected at five time points (0, 4, 8, 12 and 72 hours). For each scenario we considered eight levels of measurement noise. The ladder was used to estimate the upper limit of heterogeneity in enhancer activation signals supporting this approach. In addition, we introduced additional variability between the data sets by drawing the model parameters from normal distributions with fixed means shown in Table 2 and five percent coefficient of variation. This leads to heterogeneous data

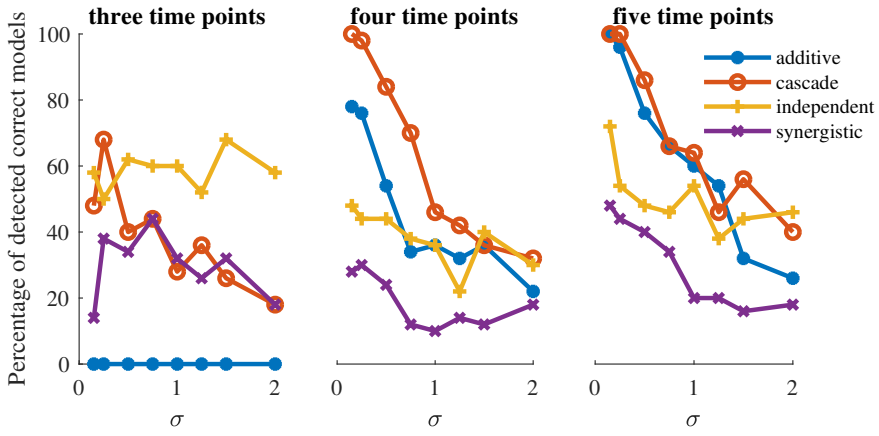

Fig. 2. Y axis shows the percentages of successful model selections, meaning that the correct model has the top rank (i.e. the highest marginal likelihood) for a given data. X axis shows tested measurement noise variances. 50 data sets are analyzed for each model and noise variance value. Model parameters, initial values and measurement noise variance were all inferred from simulated data.

containing dynamics of varying rates. In total, we created independently 4800 different data sets.

We evaluated the model selection in two settings. First one was designed to be as flexible as possible. Model parameters, initial values and measurement noise variance were all inferred from simulated data. The rate parameters were constrained to the range $[10^{-3}, 100]$, initial values at range $[0.05, 0, 5]$ and standard deviations $[0.05, 3]$. Model selection is shown in Figure 2. Not surprisingly model selection is relatively unreliable with three times points. Yet, with four time points cascade model starts to become recognizable, when measurement noise is reasonable small (standard deviation less than, say, 1). Using five measurement times enables reliable model selection for cascade and additive models. However, it is difficult for this framework to identify the correct model from very limited amounts of data when synergistic model is used to generate the data. Moreover, the framework with this amount of flexibility, seems to favour models with some dependencies between the enhancer activation signals even when data is created from models consisting independent variables.

The other setting is more rigid. In this scenario, only rate parameters are inferred from the data while initial values and values for measurements noise are fixed to the correct values. In experimental work, it may be difficult to fix these parameters to exactly correct values, but it increases the number of data points relative to the number of inferred parameters making model ranking theoretically more sound. Model selection results are shown in Figure 3. The pattern is similar to the previous case where data from three or four time points were not sufficient to trace the correct model whereas model ranking starts to become more accurate when data is available from five time points.

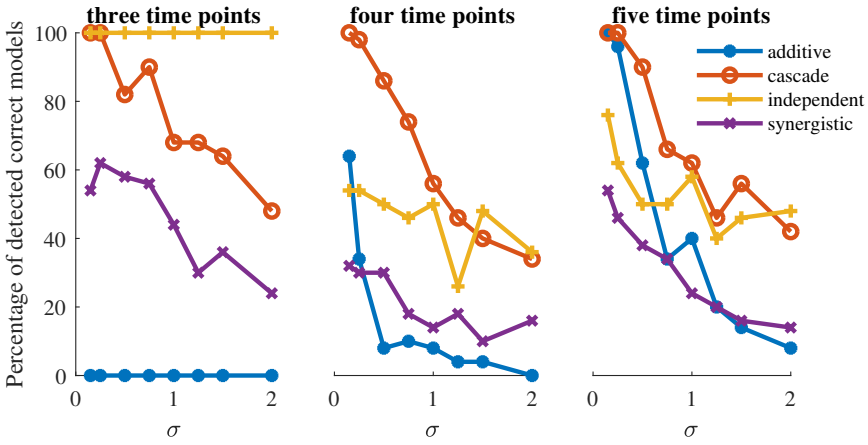

Fig. 3. Y axis shows the percentages of successful model selections, meaning that the correct model has the top rank (i.e. the highest marginal likelihood) for a given data. X axis shows tested measurement noise variances. 50 data sets are analyzed for each model and noise variance value. Model parameters were inferred from simulated data while initial values and measurement noise variance were set to correct value.

We assessed the uncertainties in the estimated parameter values of the models with parameter identifiability analysis by using the profile likelihood method [11]. The parameter profile likelihood for lth parameter of model $\mathcal{M}_k$ is defined by maximum likelihood

$$\mathrm{PL}_{\theta_{kl}}(c) = \max_{\boldsymbol{\theta}_k \in \{\boldsymbol{\theta}_k | \theta_{kl} = c\}} \log p\left(\mathcal{D} | \boldsymbol{\theta}_k, \mathcal{M}_k\right). \tag{6}$$

The profile likelihood determines confidence intervals for estimated parameter values given a fixed confidence level [11, 15]. Profile qualifies whether the parameter is identifiable or not. There are three basic categories for parameter identifiability. Clean, smooth profile with obvious maximum which furthermore has reasonably constrained confidence interval is clearly identifiable. A flat profile leads to an infinite confidence interval indicating structural non-identifiability whereas a confidence interval constrained only at one end is practically non-identifiable.

As a likelihood based method identifiability analysis clearly depends on both data and measurement noise. We applied profile likelihoods to simulated data containing five time points where measurement noise has standard deviation 0.15. With this kind of data, parameters were generally identifiable for all models except for synergistic model family. Figure 4 illustrates this case. Even then most of the parameters were identifiable. Surprisingly, parameters of a synergistic model calibrated to data derived from cascade model were all identifiable. Moreover, the same model calibration applied to additive model resulted in one practically non-identifiable parameter while others were indentifiable. Together, the results indicate that the inference framework performs well and model ranking is promisingly powerful.

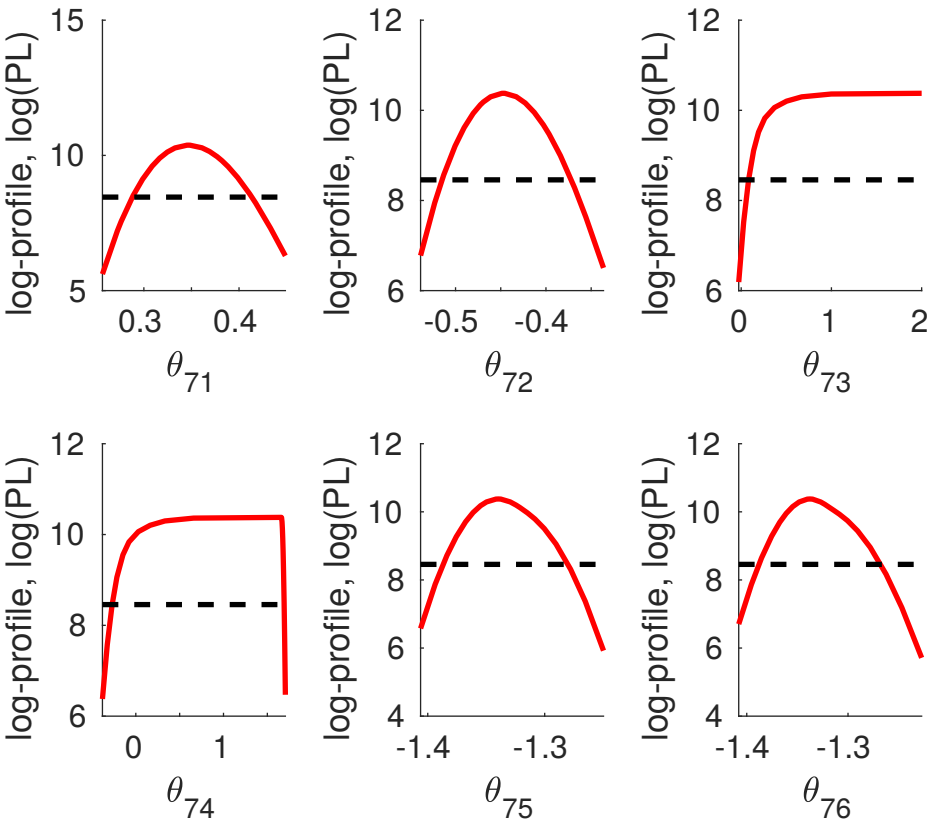

Fig. 4. The red curves represent the profile likelihoods of the kinetic parameters $\boldsymbol{\theta}_7$ represented in base 10 logarithmic scale. The dashed lines show the 95% confidence interval thresholds. The synergistic multiplicative model (model 7, Table 1.) was calibrated to data generated with the same model. Basal activation rate θ_{71} and deactivation rate θ_{72} define independent dynamics for the first activation signal x. Similarly, θ_{73} and θ_{74} control the dynamics of the second signal y. Signals x and y together drive the dynamics of z multiplicatively using parameter θ_{75} whereas θ_{76} is the deactivation rate of z. While other parameters are indentifiable, θ_{73} and θ_{74} are practically unidentifiable.

4 Discussion

We propose a new computational framework which is based on network inference, representative systems of ODEs, parameter estimation and model ranking to infer and predict enhancer activation dynamics mechanistically. We verify that a feasible amount of data is able to distinguish different models by creating synthetic data that describes different kinds of dynamics and sample data points to simulate data from wet-lab experiments. When the data is sampled in time

points that reflect well the dynamic changes in enhancer activation, the correct model family can be found with only five time points.

In this work, we concern the dynamics of an enhancer activation. The networks involved consist only the best known histone modifications and one TF factor binding. The networks can be easily expanded to contain other histone modifications, TF binding or other molecules as well. In that case, it is important to have sufficient amount of abundance data from the new components and consider the possible mechanisms the components can impact to the system. It may be that new terms representing for example repressive effect to the systems needs to be introduced to the ODEs. For all expansions detailed attention should be paid to the experimental design and to the time scale of the studied phenomenon.

Unlike previous methods used to infer causal relations between molecules engaged in enhancer activation, the suggested method utilizes more effectively time evolution of abundance data. Instead of snapshots or series of snapshots the occasional relations captured by for example (dynamic) Bayesian networks, the proposed approach combines all information into a single complete causal model of dynamic relations between the molecules. In addition, mechanistic modeling enables us to predict the (relative) abundances of the molecules.

5 Conclusion

We have represented the first mathematical model to assess dynamic causal dependencies between key molecular components during cell type specific enhancer activation. This approach enables both predictions of the dynamics and causality inference between the activation events going beyond previously available methods detecting only static features. The introduced method works well with data from a few time points and hence is applicable in both designing time course experiments and analyzing experimental data studies.

Funding

This work has been supported by the Academy of Finland, project 275537 and Chan Zuckerberg Initiative.

Appendix

Table 2. The simulated models and the means of the parameters used in data simulations. One representative from each model family were selected for generating data. Index $k \in \{0, 1, 7, 11\}$ specifies the model structure as described in Table 1. A sampled parameter vector $\boldsymbol{\theta}_k$ consists of kinetic parameters θ_{kl}, initial values for three ordered enhancer activation signals denoted by x_0, y_0 and z_0 and the simulation specific measurement noise σ_s which was 0.15, 0.25, 0.5, 0.75, 1, 1.25 1.5 or 2.0. Independent, cascade and synergistic models have six kinetic parameters. Consecutive odd and even elements are the activation rates and the corresponding deactivation rates of the enhancer activation signal, respectively. Additive models have seven kinetic parameters. First four of them are the basal activation and the deactivation rates of enhancer activity signal x and y mediating dynamics independent from other variables while θ_{k5} and θ_{k6} are the activation rates of z activation caused by x and y and θ_{k7} is the deactivation rate of z.

model	k	θ_{k1}	θ_{k2}	θ_{k3}	θ_{k4}	θ_{k5}	θ_{k6}	θ_{k7}	x_0	y_0	z_0	σ
independent	0	3.1	.3	3.1	.3	3.1	.3		0.03	0.02	0.04	σ_s
cascade	1	3.1	.3	.3	.25	.9	1		0.03	0.02	0.04	σ_s
synergistic	7	2.4	.4	2	1	0.05	.05		0.03	0.02	0.04	σ_s
additive	11	3.1	.3	.2	0.01	.9	0.7	1	0.03	0.02	0.04	σ_s

Acknowledgements

We acknowledge the computational resources provided by Aalto Science-IT project.

References

1. Bishop, C.M.: Pattern Recognition and Machine Learning (Information Science and Statistics). Springer-Verlag, Berlin, Heidelberg (2006)
2. Calo, E., Wysocka, J.: Modification of enhancer chromatin: what, how, and why? Molecular cell **49**(5), 825–837 (2013)
3. Creyghton, M.P., et al.: Histone h3k27ac separates active from poised enhancers and predicts developmental state. Proceedings of the National Academy of Sciences **107**(50), 21931–21936 (2010)
4. Friel, N., Wyse, J.: Estimating the evidence–a review. Statistica Neerlandica **66**(3), 288–308 (2012)
5. Fröhlich, F., Kaltenbacher, B., Theis, F.J., Hasenauer, J.: Scalable parameter estimation for genome-scale biochemical reaction networks. PLoS computational biology **13**(1), e1005331 (2017)
6. Gelman, A., et al.: Bayesian data analysis, vol. 2. Chapman & Hall/CRC, second edition edn. (2004)
7. Ghavi-Helm, Y., et al.: Enhancer loops appear stable during development and are associated with paused polymerase. Nature **512**(7512), 96–100 (2014)

8. Girolami, M.: Bayesian inference for differential equations. Theoretical Computer Science **408**(1), 4–16 (2008)
9. Hayashi, Y., et al.: Theoretical framework for the histone modification network: modifications in the unstructured histone tails form a robust scale-free network. Genes to Cells **14**(7), 789–806 (2009)
10. Heintzman, N.D., et al.: Distinct and predictive chromatin signatures of transcriptional promoters and enhancers in the human genome. Nature genetics **39**(3), 311–318 (2007)
11. Kreutz, C., Raue, A., Kaschek, D., Timmer, J.: Profile likelihood in systems biology. The FEBS journal **280**(11), 2564–2571 (2013)
12. Lasserre, J., et al.: Finding associations among histone modifications using sparse partial correlation networks. PLoS computational biology **9**(9), e1003168 (2013)
13. Le, N.T., Ho, T.B.: Reconstruction of histone modification network from next-generation sequencing data. In: Bioinformatics and Bioengineering (BIBE), 2011 IEEE 11th International Conference on. pp. 181–188. IEEE (2011)
14. Maier, E., et al.: Stat6-dependent and-independent mechanisms in th2 polarization. European journal of immunology **42**(11), 2827–2833 (2012)
15. Meeker, W.Q., Escobar, L.A.: Teaching about approximate confidence regions based on maximum likelihood estimation. The American Statistician **49**(1), 48–53 (1995)
16. Natoli, G.: Maintaining cell identity through global control of genomic organization. Immunity **33**(1), 12–24 (2010)
17. Oki, S., Otsuki, N., Kohsaka, T., Azuma, M.: Stat6 activation and th2 cell proliferation driven by cd28 signals. European journal of immunology **30**(5), 1416–1424 (2000)
18. Perner, J., et al.: Inference of interactions between chromatin modifiers and histone modifications: from chip-seq data to chromatin-signaling. Nucleic acids research **42**(22), 13689–13695 (2014)
19. Raue, A., Schilling, M., Bachmann, J., Matteson, A., Schelke, M., Kaschek, D., Hug, S., Kreutz, C., Harms, B.D., Theis, F.J., et al.: Lessons learned from quantitative dynamical modeling in systems biology. PloS one **8**(9), e74335 (2013)
20. Raue, A., Steiert, B., Schelker, M., Kreutz, C., Maiwald, T., Hass, H., Vanlier, J., Tönsing, C., Adlung, L., Engesser, R., et al.: Data2dynamics: a modeling environment tailored to parameter estimation in dynamical systems. Bioinformatics **31**(21), 3558–3560 (2015)
21. Schwarz, G.: Estimating the dimension of a model. The annals of statistics **6**(2), 461–464 (1978)
22. Stapor, P., Weindl, D., Ballnus, B., Hug, S., Loos, C., Fiedler, A., Krause, S., Hro, S., Frhlich, F., Hasenauer, J.: Pesto: Parameter estimation toolbox. Bioinformatics **34**(4), 705–707 (2018). https://doi.org/10.1093/bioinformatics/btx676, http://dx.doi.org/10.1093/bioinformatics/btx676
23. Vahedi, G., et al.: Stats shape the active enhancer landscape of t cell populations. Cell **151**(5), 981–993 (2012)
24. Voss, T.C., Hager, G.L.: Dynamic regulation of transcriptional states by chromatin and transcription factors. Nature Reviews Genetics **15**(2), 69–81 (2014)
25. Yu, H., et al.: Inferring causal relationships among different histone modifications and gene expression. Genome research **18**(8), 1314–1324 (2008)
26. Zhou, J., Troyanskaya, O.G.: Global quantitative modeling of chromatin factor interactions. PLoS Comput. Biol **10**, e1003525 (2014)